EPRI | ELECTRIC POWER RESEARCH INSTITUTE

Program on Technology Innovation: Use of CAV in Determining Effects of Small Magnitude Earthquakes on Seismic Hazard Analyses

1012965

Program on Technology Innovation: Use of Minimum CAV in Determining Effects of Small Magnitude Earthquakes on Seismic Hazard Analyses

1012965

Technical Update, December 2005

EPRI Project Managers
R. Kassawara
L. Sandell

Cosponsor
U.S. Department of Energy
Office of Nuclear Energy
Sciences & Technology
19901 Germantown Road, NE-20
Germantown, MD 20874-1290

ELECTRIC POWER RESEARCH INSTITUTE
3420 Hillview Avenue, Palo Alto, California 94304-1395 ▪ PO Box 10412, Palo Alto, California 94303-0813 ▪ USA
800.313.3774 ▪ 650.855.2121 ▪ askepri@epri.com ▪ www.epri.com

DISCLAIMER OF WARRANTIES AND LIMITATION OF LIABILITIES

ORGANIZATION(S) THAT PREPARED THIS DOCUMENT

ARES Corporation, Inc.

This is an EPRI Technical Update report. A Technical Update report is intended as an informal report of continuing research, a meeting, or a topical study. It is not a final EPRI technical report.

NOTE

For further information about EPRI, call the EPRI Customer Assistance Center at 800.313.3774 or e-mail askepri@epri.com.

CITATIONS

This document was prepared by

ARES Corporation, Inc.
5 Hutton Centre Drive
Suite 610
Santa Ana, CA 92707

Norm A. Abrahamson, Inc.
152 Dracena Avenue
Piedmont, CA 94611

Principal Investigators
N. Abrahamson
J. Watson-Lamprey

ARES Corporation, Inc.
5 Hutton Centre Drive
Suite 610
Santa Ana, CA 92707

Principal Investigators
G. Hardy
K. Merz

This document describes research sponsored by the Electric Power Research Institute (EPRI) and the U.S. Department of Energy under Award No. (DE-FC07-04ID14533). Any opinions, findings, and conclusions or recommendations expressed in this material are those of the author(s) and do not necessarily reflect the views of the Department of Energy.

This publication is a corporate document that should be cited in the literature in the following manner:

Program on Technology Innovation: Use of Minimum CAV in Determining Effects of Small Magnitude Earthquakes on Seismic Hazard Analyses. EPRI, Palo Alto, CA and the U.S. Department of Energy: 2005. 1012965.

ABSTRACT

This study provides the technical basis for establishing the appropriate distribution of low magnitude earthquakes for use in probabilistic seismic hazard computations for nuclear power plant applications. Current seismic hazard methods generally utilize a lower bound body wave magnitude cut-off value of 5.0 (approximate moment magnitude of 4.6) to integrate the probabilistic seismic hazard. This lower bound magnitude cut-off level was a conservatively defined value based on several past EPRI research studies whose objective was to estimate the damage potential of small earthquakes for probabilistic seismic hazard analysis. Other research has been conducted by EPRI to determine the single ground motion measure that is best correlated with potential damage. Several ground motion measures such as peak ground acceleration, Arias intensity, root mean square acceleration, and cumulative absolute velocity (CAV) were evaluated in the process of selecting the best parameter for use in predicting the threshold of potential damage. The CAV was determined to be the best parameter and a CAV value of 0.16 g-sec was found to be a conservative characterization of the threshold between damaging earthquake motions and non-damaging earthquake motions for buildings of good design and construction as defined by the Modified Mercalli Scale. In this study, a model for CAV is developed using strong motion data from the western United States (WUS) in two steps. In the first step, CAV is modeled as a function of the uniform duration, magnitude, peak ground acceleration, and site shear wave velocity. In the second step, the uniform duration is modeled as a function of the peak ground acceleration, magnitude, and site shear wave velocity. Taken together, these two steps lead to a model of CAV that depends on parameters that are available in a standard PSHA. Comparisons with a small set of ground motions from earthquakes in the central and eastern United States (CEUS) and Canada show that the CAV model and the duration model developed from the WUS data sets are applicable to the CEUS earthquakes. An example application of the CAV filtering to seismic hazard in the EUS is shown. The application of a minimum CAV value significantly reduces the contribution of small magnitude earthquakes to the total hazard. The magnitude of the dominant earthquake increases from 5.25 to 5.8 by applying the minimum CAV. This example shows that the past PSHA studies that used a minimum moment magnitude of 4.6 can overestimate the hazard by including earthquakes that are not damaging, but may contribute significantly to the hazard when they are located at short distances from the site.

CONTENTS

LIST OF FIGURES

LIST OF TABLES

1
INTRODUCTION

Probabilistic seismic hazard analysis (PSHA) for a site integrates the hazard from all possible earthquakes in the site region that are potentially damaging. In current practice, non-damaging earthquakes are those with magnitudes below a conservatively determined lower bound earthquake magnitude. For these applications, earthquakes above the minimum magnitude are considered to be potentially damaging, and earthquakes below the minimum magnitude are not potentially damaging. This lower bound is included in the PSHA by setting the minimum magnitude in the hazard integral as shown in eq. 1-1.

$$\nu(Sa > z) = \sum_{i=1}^{N_{source}} N_i(M > M_{\min}) \int_{M_{\min}}^{M_{\max i}} \int_{0}^{\infty} f_{mi}(M)\, f_{ri}(r,M)\, P(Sa > z \mid M,r)\, dr\, dM \quad \textbf{(Equation 1-1)}$$

where $\nu(Sa>z)$ is the hazard, f_m and f_r are probability density functions describing the distributions of earthquake magnitudes and distances, respectively, and $N_i(M>M_{min})$ is the rate of earthquakes for the i^{th} source.

The bounding lower bound magnitude approach has important negative impact on hazard, causing a bias to high hazard particularly for higher response spectra frequencies. The bias is a consequence of incorporating non-damaging earthquakes into the hazard. These are primarily small magnitude events near the site of interest, which occur with much greater frequency because of the exponential increase in the number of earthquakes with decreasing magnitude. As an example, using a minimum moment magnitude of 4.6, the deaggregation of the $2x10^{-5}$/yr hazard for a rock site located in Virginia, away from the Charleston and New Madrid sources, is shown in Figure 1-1.

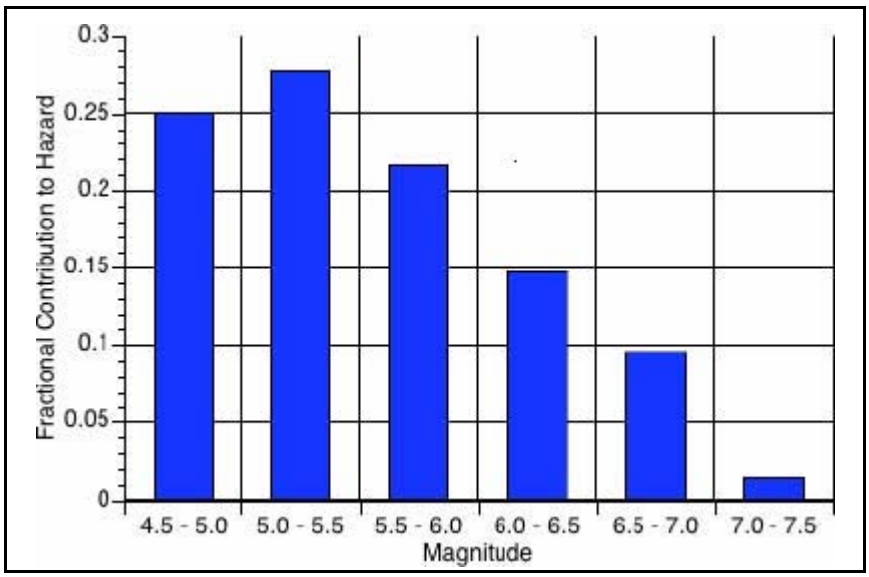

Figure 1-1
Example of Deaggregation for EUS Source Zones
There is a large contribution to the hazard from earthquakes near the M=4.6 lower bound magnitude.

There is a large contribution from events with magnitudes just above the minimum magnitude, causing the computed hazard and the determination of the controlling earthquake to be biased to a smaller magnitude and closer distance. A summary of approaches to determining appropriate minimum magnitude to use for buildings of good design and construction as defined by the Modified Mercalli Scale is given in McCann and Reed (1989). Based on that early work, a conservative assumption is that for buildings of good design and construction, a minimum body wave magnitude of 5.0 should be used for PSHA In the recent EPRI sponsored PSHA for nuclear power plants in the EUS, a minimum m_{bLG} of 5.0 was used. This minimum m_{bLG} was converted to a minimum moment magnitude of 4.6.

The lower bound magnitude approach used in past seismic hazard modeling, eq. 1-1, is equivalent to assuming that the probability of an earthquake being potentially damaging is a step function. For example, if the minimum moment magnitude is 4.6, then a moment magnitude 4.61 has a probability of 1.0 of being potentially damaging, whereas a moment magnitude 4.59 has a probability of 0.0 of being potentially damaging. Clearly, the step function is not realistic and does not properly represent the potential for damage as a function of earthquake magnitude. The transition from not potentially damaging to potentially damaging should be a smoother distribution on magnitude.

As an alternative to using earthquake magnitude to determine non-damaging earthquakes, Reed and Kennedy (1988) proposed using the ground motion measure, CAV, given by the integral of the absolute value of a ground motion acceleration recording. To make the CAV value representative of strong ground shaking rather than coda waves (small amplitudes that can continue on for a long time after the strong shaking), O'Hara and Jacobson (1991) restricted the integration for computing CAV to 1-second time windows that have amplitudes of at least 0.025g. This definition of CAV is given by:

$$CAV = \sum_{i=1}^{N} H(pga_i - 0.025) \int_{t=t_i}^{t_{i+1}} |a(t)| dt \qquad \textbf{(Equation 1-2)}$$

where N is the number of 1-second time windows in the time series, pga_i is the peak ground acceleration in time window i, t_i is the start time of time window i, and H(x) is the Heaviside function (unity for x>0 and 0 otherwise).

By evaluating dependence of CAV of earthquake magnitude and measures of ground motion, a distribution on potentially damaging earthquakes is developed. In this report, we develop a model for estimating the CAV and show how to use the probability of exceeding a CAV value of 0.16 g-sec is used to remove earthquakes that are not potentially damaging from the hazard analysis. A model for CAV is needed because the PSHA calculation does not use time histories directly.

2
EMPIRICAL MODEL OF CAV

In this section, we derive empirical models for the CAV based on the extensive WUS strong motion data set. We then check the applicability of these WUS based CAV models against strong motion data from EUS earthquakes and adjust the WUS model as needed.

Empirical Data Set for WUS

The PEER NGA data set (PEER 2005) consists of 3551 recordings (mostly 3-component) from 173 earthquakes in active shallow crustal regions of the world. From this full dataset, recordings from individual earthquakes and recording stations were removed if the data were considered to be unreliable or not applicable to the WUS. In addition, components with PGA<0.025g were removed since these have zero CAV by definition. The resulting data set consists of 4,422 horizontal components from 97 earthquakes. The WUS data set used for developing the CAV model is given in the file "CAV_WUS_DATA.XLS," which is included on the enclosed CD-ROM.

The distribution of the earthquake moment magnitudes and rupture distances from the subset of WUS data used to develop the CAV is shown in Figure 2-1. The data are primarily from earthquakes with moment magnitudes greater than 5.0. The distribution of the average shear-wave velocity in the top 30 m, V_{S30}, is shown in Figure 2-2. This figure shows that only a small fraction of the recordings are for hard rock conditions (e.g., V_{S30}>1000 m/s) that are typically used for the EUS.

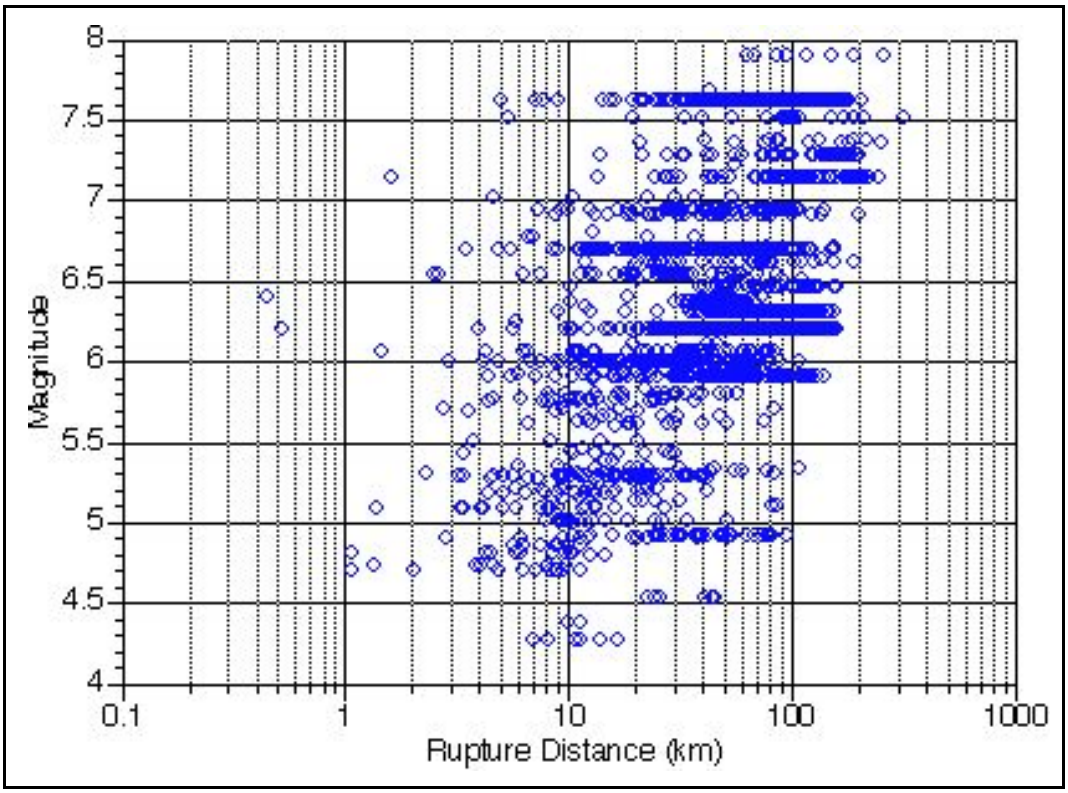

Figure 2-1
Distribution of Earthquake Magnitudes and Distances for the WUS Data Set

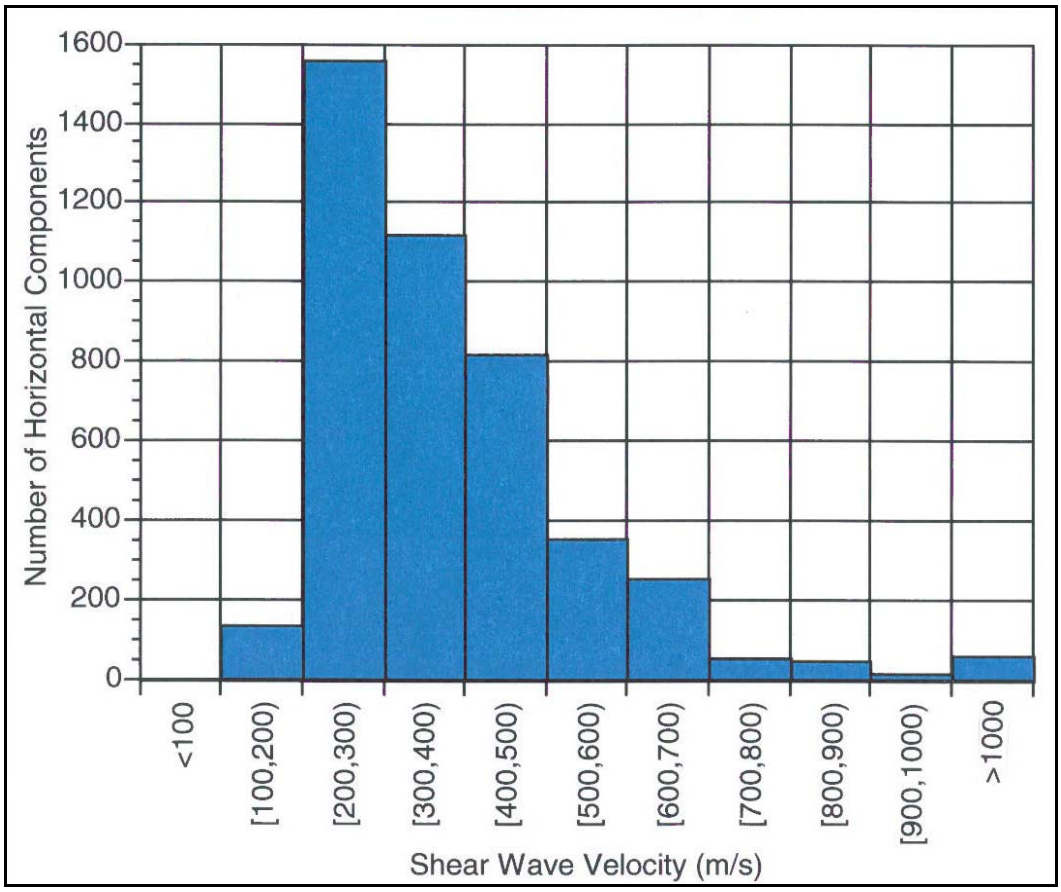

Figure 2-2
Distribution of V_{S30} Values for the WUS Data Set

Empirical Data Set for EUS

There are few strong motion data from CEUS earthquakes. EPRI (1993) compiled a list of ground motions recorded by CEUS and Canadian earthquakes through 1991. The earthquakes with $M \geq 4$ from the EPRI (1993) study are listed in Table 2-1. For the comparison with the WUS CAV models, only data with PGA values greater than 0.03g were used since the CAV is highly variable for recordings with PGA values close to the 0.025g threshold and these recordings are excluded. Only 9 of the 16 earthquakes had at least one horizontal component of ground motions with a PGA greater than 0.03g. The recordings with horizontal PGAs greater than 0.025g are listed in Table 2-2. The EUS data is given in the file "CAV_EUS_DATA.XLS," which is included on the enclosed CD-ROM.

Table 2-1
CEUS and Canadian Earthquakes with M ≥ 4 from the EPRI (1993) Strong Motion Data Set
The EPRI data set covers 1976-1991

EQID	Earthquake Name	Date	Hr	Min	Sec	M	m_{Lg}	Number of Horizontal Components With PGA > 0.03g
NM760300	New Madrid	1976.03.25	0	41	20.50	4.6		1
NM760301	New Madrid	1976.03.25	1	0	11.90	4.2		0
NB820100	New Brunswick (A5)	1982.01.11	21	41	8.00	5.2	5.5	0
FK820100	Franklin Falls, New Hampshire	1982.01.19	0	14	42.00	4.3	4.8	7
NB820300	New Brunswick (A13)	1982.03.31	21	2	20.40	4.0	4.8	12
NB820600	New Brunswick (A19)	1982.06.16	11	43		4.0	4.6	0
GN831000	Goodnow, NY	1983.10.07	10	18	46.00	4.8		0
NH851100	Nahanni, CAN (F1)	1985.11.09	4	46		4.6		2
NH851200	Nahanni, CAN	1985.12.23	5	16	6.00	6.7		6
NH851201	Nahanni, CAN (A1)	1985.12.25	15	42		5.0		2
NO860100	Northeastern Ohio	1986.01.31	16	46	42.3	4.6	5.0	2
SG881100	Saguenay, CAN (F1)	1988.11.23	9	11	27.30	4.5	4.8	0
SG881101	Saguenay, CAN	1988.11.25	23	46	4.50	5.9	6.5	20
NM890400	New Madrid	1989.04.27	16	47	49.80	4.7	4.7	0
CG900900	Cape Girardeau	1990.09.26	13	18	51.30		5.0	0
NM910501	New Madrid	1991.05.04	1	18	54.60	4.4	4.7	2

Table 2-2
Ground Motions from the EPRI (1993) CEUS Database With at Least One Horizontal Component with PGA>0.025g

EQID	M	Station Name	Distance (km)	Vs30 (m/s)	Comp H1	Comp H2	PGA H1 (g)	PGA H2 (g)	Used in Current Study?
NM760300	4.6	2444B	12.7	300	208	118	0.041	0.022	No*
FK820100	4.3	2627A	8.3	350	225	135	0.143	0.385	Yes
FK820100	4.3	2627B	8.3	600	045	315	0.293	0.550	Yes
FK820100	4.3	2632C	62	350	245	155	0.038	0.023	Yes
FK820100	4.3	2604	61	1500	270	180	0.015	0.032	Yes
FK820100	4.3	2630B	76	2000	275	185	0.032	0.023	Yes
NB820300	4.0	HL	7.5	600	018	288	0.181	0.346	Yes
NB820300	4.0	MR	5.7	2000	028	118	0.152	0.235	Yes
NB820300	4.0	LL	7.2	600	099	189	0.297	0.575	Yes
NB820300	4.0	IB	5.0	600	231	321	0.425	0.413	Yes
NB820300	4.0	HCL	5.7	600	099	189	0.397	0.186	No*
NB820300	4.0	IB2	4.1	2000	321	231	0.289	0.341	No*
NH851100	4.6	6098	8.1	660	240	330	0.460	0.382	Yes
NH851200	6.7	6097	6.0	660	010	280	1.101	1.345	Yes
NH851200	6.7	6098	8.0	660	330	240	0.390	0.545	Yes
NH851200	6.7	6099	16.0	660	360	270	0.194	0.186	Yes
NH851201	5.0	6099	19.2	660	270	360	0.089	0.105	Yes
NO860100	4.6	PPBF	19.6	300	180	270	0.179	0.100	Yes
SG881101	5.9	GSC1	118	2000	000	270	0.121	0.097	Yes
SG881101	5.9	GSC2	167	1500	051	321	0.051	0.051	Yes
SG881101	5.9	GSC5	113	2000	097	007	0.027	-	Yes
SG881101	5.9	GSC7	96	350	175	085	0.125	0.174	Yes
SG881101	5.9	GSC8	98	1500	063	333	0.124	0.060	Yes
SG881101	5.9	GSC9	132	1500	000	270	0.046	0.056	Yes
SG881101	5.9	GSC10	118	1500	000	270	0.040	0.057	Yes
SG881101	5.9	GSC16	52	2000	214	124	0.107	0.131	Yes
SG881101	5.9	GSC17	70	2000	000	270	0.156	0.091	Yes
SG881101	5.9	GSC20	95	2000	000	270	0.125	0.102	Yes
NM910501	4.7	RSCO	7.6	300	000	090	0.127	0.098	No*

* Time histories not readily available

Model for CAV Including Duration Dependence

The CAV was calculated for the horizontal components from ground surface records in the NGA PEER data set. The resulting CAV values are shown in Figure 2-3 as a function of the PGA. Figure 2-3 shows that the CAV depends on the peak acceleration and earthquake magnitude, but there is large scatter. Given the definition of CAV in eq. 1-2, CAV will depend strongly on the duration of strong shaking. In this study, we use the uniform duration (Bolt, 1973) defined as the total time during which the absolute value of the acceleration time series exceeds a specified threshold, herein defined as 0.025g. Figure 2-4 shows that the uniform duration is a much better predictor of CAV than the PGA. While the uniform duration is not directly available from the PSHA results, we chose to model CAV as a function of the uniform duration and then model the dependence of the duration on other parameters (PGA, magnitude, V_{S30}) because this provides a simple physical aspect of ground motion that can be modified for CEUS conditions. This allows the CAV model to be modified for CEUS conditions, if needed, based on differences in the duration in the WUS and CEUS.

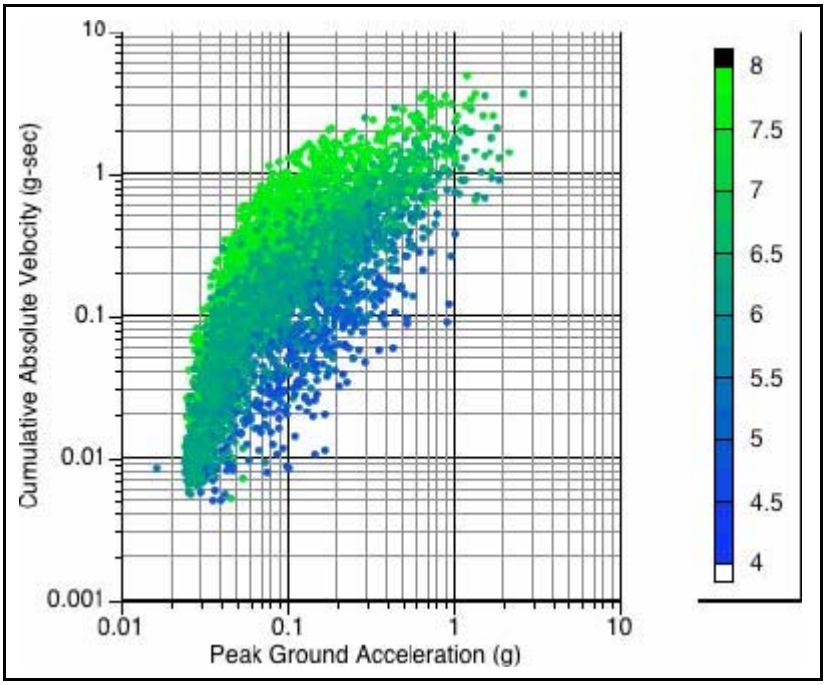

Figure 2-3
Dependence of the CAV on the PGA and Magnitude

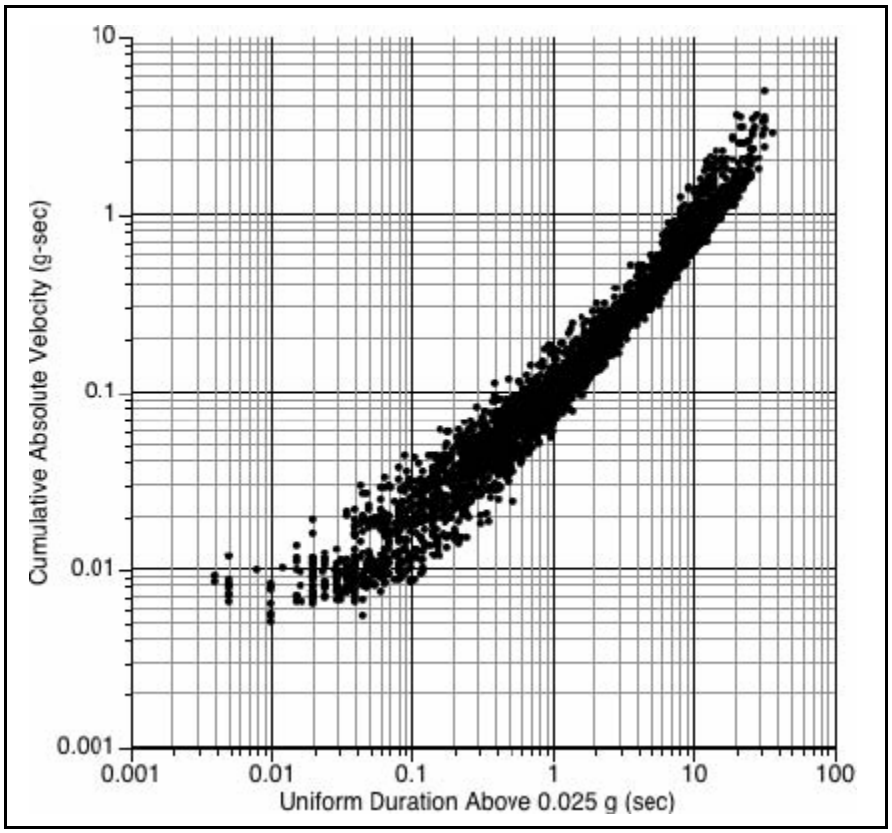

Figure 2-4
Duration Dependence of the CAV

Based on the plot of the CAV values in Figure 2-4, CAV is approximately lognormally distributed and is heteroscedastic (non-constant standard deviation) with the standard deviation decreasing with increasing duration. The standard deviation increase for smaller durations, but this range of ground motions is not important for determining if the CAV exceeds the 0.16g-sec threshold.

Based on preliminary evaluations of the CAV data, the CAV is modeled as a function of uniform duration, PGA, M, and V_{S30} using the following functional form:

$$\ln\left(CAV(g-s)\right)=\begin{cases} c_0+c_1(M-6.5)+c_2(M-6.5)^2+c_3\ln(PGA) \\ +c_4\left(\ln(PGA)\right)^2+c_5\left(\ln(PGA)\right)^3+c_6\left(\ln(PGA)\right)^4 \\ +c_7(V_{S30}-6)+c_8\ln(Dur_{uni})+c_9\left(\ln(Dur_{uni})\right)^2 & for PGA\le 1g \\ c_0+c_1(M-6.5)+c_2(M-6.5)^2+c_3\ln(PGA) \\ +c_7(V_{S30}-6)+c_8\ln(Dur_{uni})+c_9\left(\ln(Dur_{uni})\right)^2 & for PGA>1g \end{cases} \quad \textbf{(Equation 2-1)}$$

where Dur_{uni} is the uniform duration above 0.025g in sec, PGA is the peak horizontal acceleration in g, and the V_{S30} is the shear-wave velocity over the top 30m in m/s. The higher order PGA dependence was removed for PGA greater than 1g because the PGA dependence of the CAV model determined using the higher order terms had excessive curvature, causing the model for CAV to decrease when extrapolated to PGA values greater than 1g.

A regression analysis was performed using ordinary least-squares to estimate the coefficients in eq. 2-1. The resulting coefficients are listed in Table 2-3. The median CAV model is shown in Figures 2-5 and 2-6. These figures show that the CAV is only weakly dependent on PGA, magnitude, and Vs30 if the duration is known. The standard deviation ranges from 0.37 for small duration to 0.10 natural log units for large durations, which is very small for ground motion models indicating that CAV is well determined if the duration, PGA, M, and V_{S30} are known. The residuals* of the CAV model are shown as a function of duration, PGA, magnitude, and V_{S30} in Figures 2-7, 2-8, 2-9, and 2-10 respectively. These figures do not show any significant trends in the residuals.

Table 2-3
Coefficients for CAV Model

Coefficient	Estimate
C_0	-1.75
C_1	0.0567
C_2	-0.0417
C_3	0.0737
C_4	-0.481
C_5	-0.242
C_6	-0.0316
C_7	-0.00936
C_8	0.782
C_9	0.0343
$\sigma_{\ln CAV1}$	$\begin{cases} 0.37 & for Dur_{uni} < 0.2 \\ 0.37 - 0.090\left(\ln(Dur_{uni}) - \ln(0.2)\right) & for 0.2 \le Dur_{uni} \le 4 \\ 0.10 & for Dur_{uni} > 4 \end{cases}$

* Residuals are estimates of experimental error obtained by subtracting the observed responses from the predicted responses.

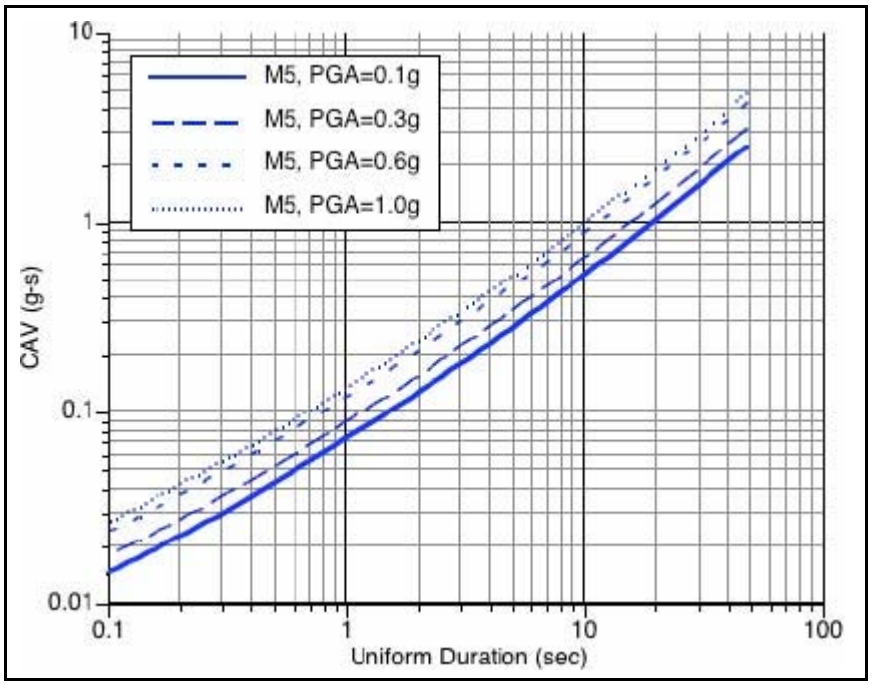

Figure 2-5
Median CAV Model for Vs= 600m/s for Different PGA Values

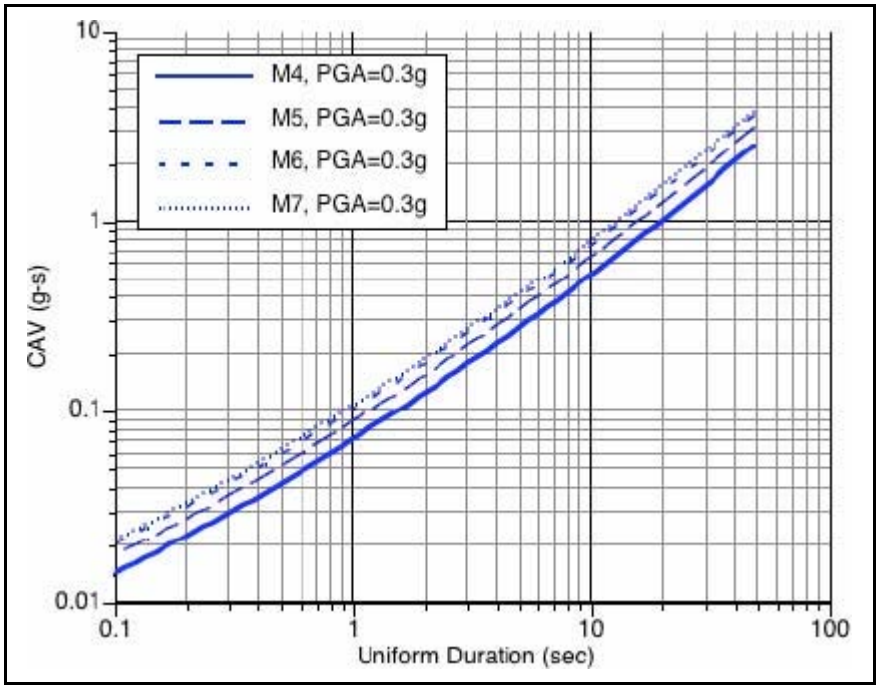

Figure 2-6
Median CAV Model for Vs=600m/s for Different Magnitudes

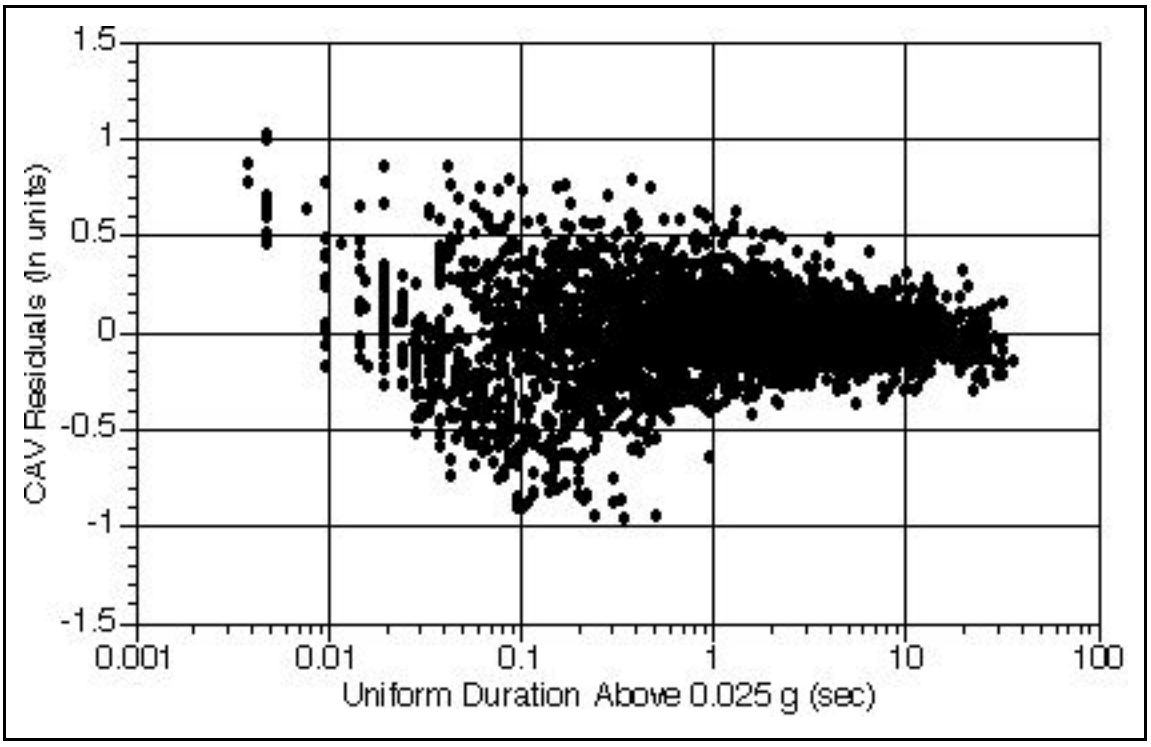

Figure 2-7
Duration Dependence of the CAV Residuals

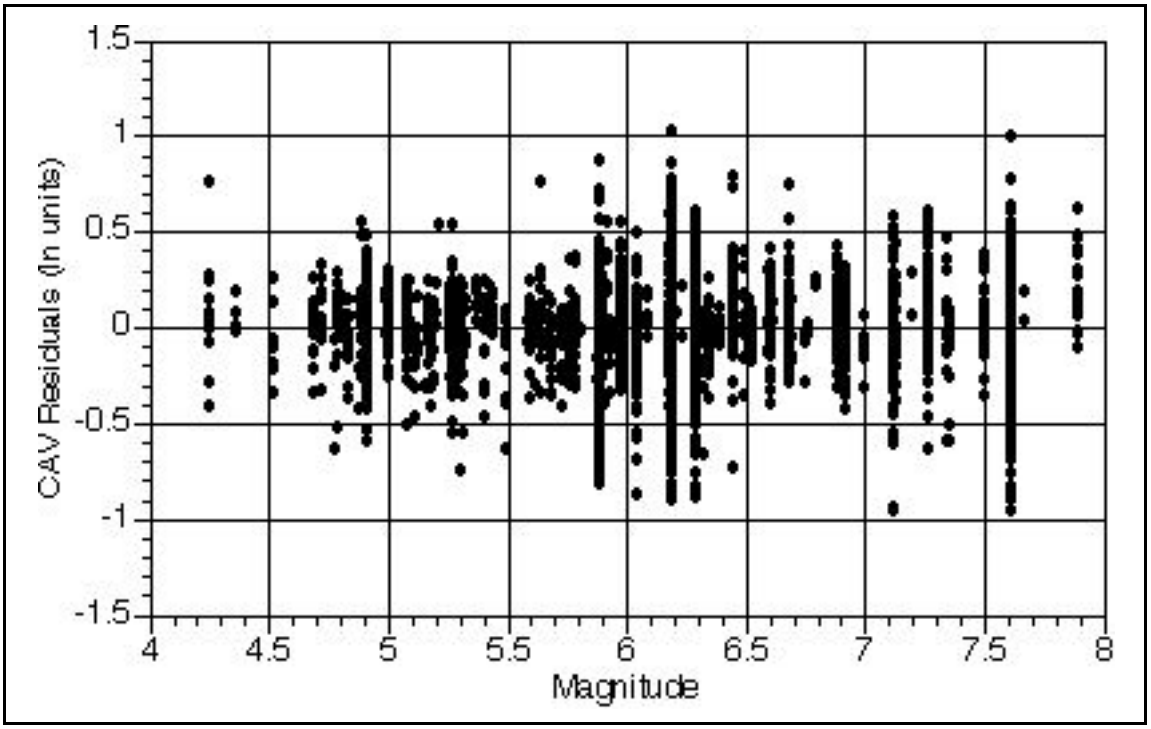

Figure 2-8
Magnitude Dependence of the CAV Residuals

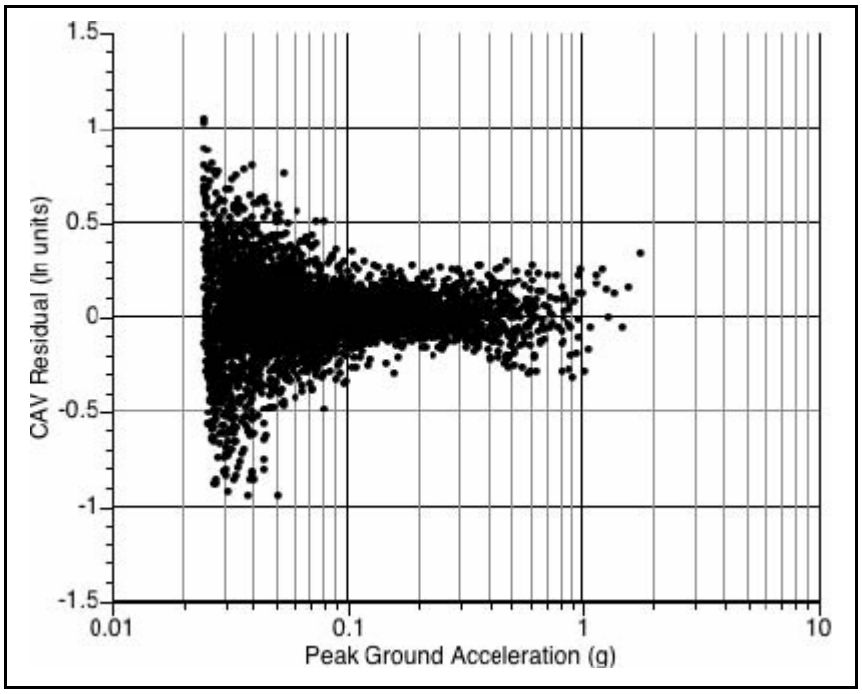

Figure 2-9
PGA Dependence of the CAV Residual

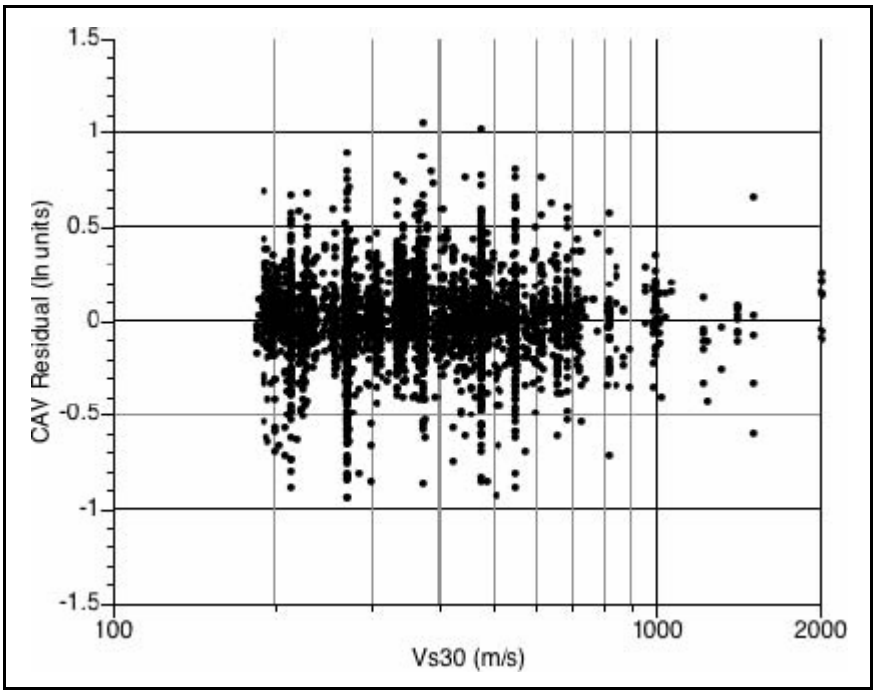

Figure 2-10
Vs30 Dependence of the CAV Residual

Using this WUS based CAV model, we then computed the residuals for ground motions from CEUS and Canadian earthquakes. The residuals, shown in Figure 2-11 as a function of the PGA, do not show a significant bias for PGA > 0.04g, indicating that the WUS CAV model is applicable to the EUS if the uniform duration of the CEUS data is known.

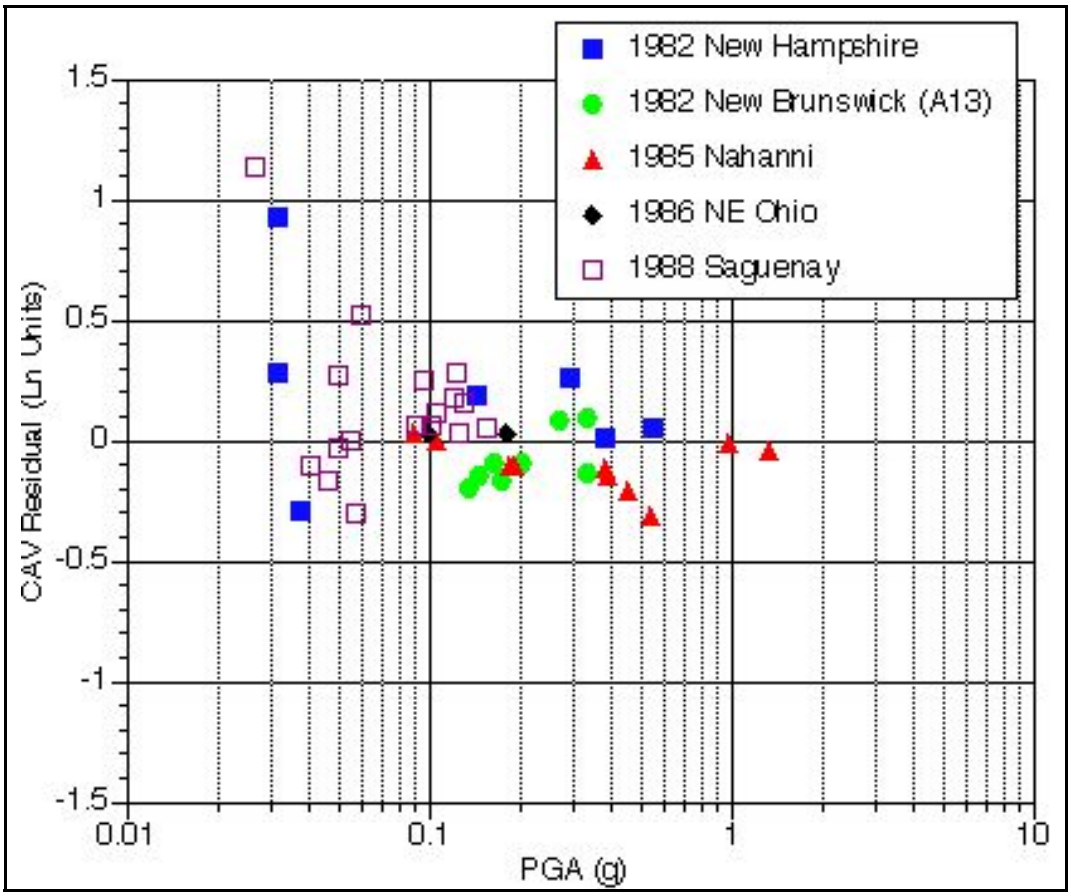

Figure 2-11
CAV Residuals for CEUS/Canadian Data Using the Observed Uniform Durations

Model for Uniform Duration

The CAV model derived in this Section includes uniform duration, a parameter that PSHA does not compute directly. To use the model to compute CAV, we need to develop a model to estimate uniform duration for the scenario events that make up the hazard curve using parameters that are available from the PSHA. A model for uniform duration above 0.025g is developed using the same WUS data set used to develop the CAV model.

The following functional form is used to model the uniform duration:

$$\ln\left(Dur_{uni}(s)\right) = a_1 + a_2 \ln(PGA) + \frac{a_3}{\ln(PGA) + a_4} + a_5(M - 6.5) + a_6(M - 6.5)^2 + a_7\left(\ln(V_{S30}) - 6\right) \quad \textbf{(Equation 2-2)}$$

The coefficients computed using ordinary least-squares are listed in Table 2-5. The standard deviation is 0.51. The resulting median duration is shown as a function of the PGA for different magnitudes in Figure 2-12. The residuals of uniform duration model using the WUS data are shown in Figures 2-13, 2-14, 2-15, and 2-16 for PGA, magnitude, distance, and V_{S30}, respectively. These figures do not show any significant trends in the residuals.

Table 2-4
Coefficients for Uniform Duration Model

Coefficient	WUS Model (Eq. 2-2)
a_1	3.50
a_2	0.0714
a_3	-4.19
a_4	4.28
a_5	0.733
a_6	-0.0871
a_7	-0.355
$\sigma_{\ln DUR}$	0.509

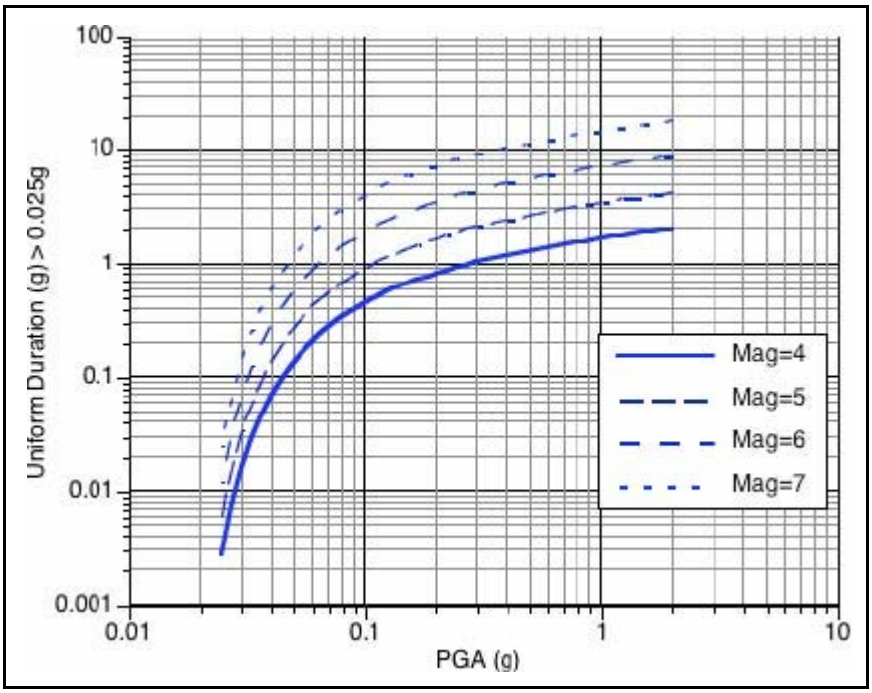

Figure 2-12
Median Uniform Duration for Vs30=600

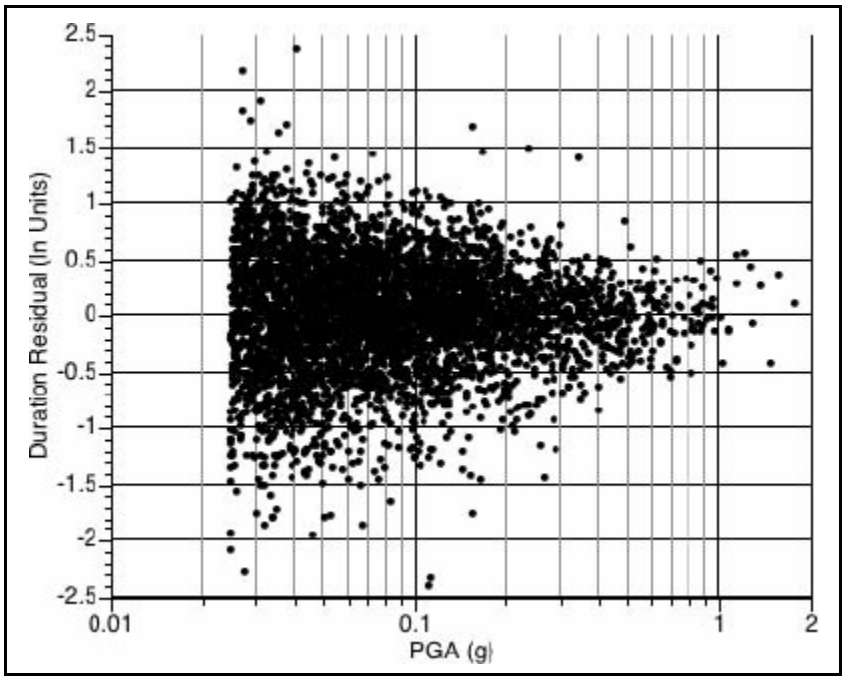

Figure 2-13
PGA Dependence of the Uniform Duration Residuals

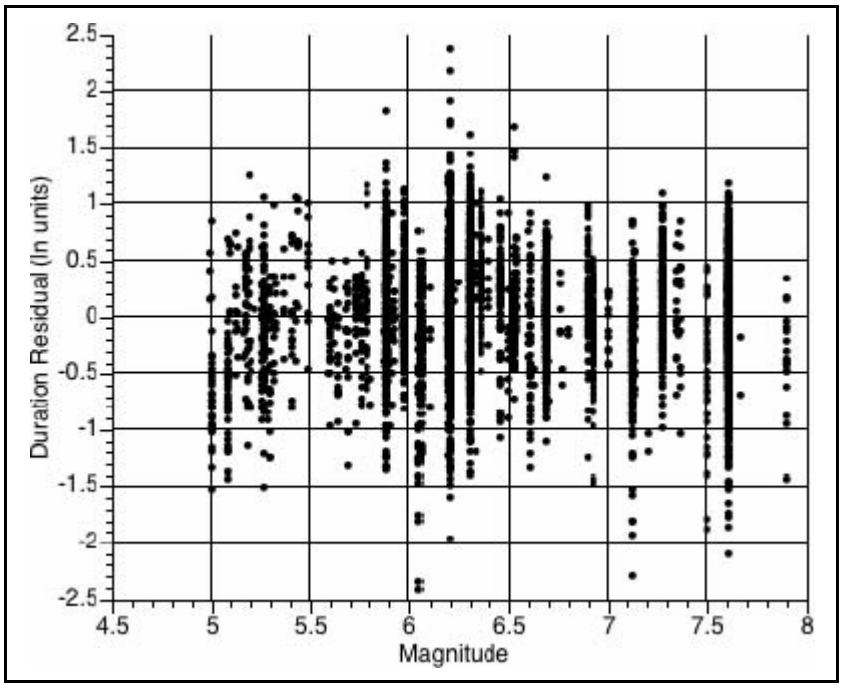

Figure 2-14
Magnitude Dependence of the Uniform Duration Residuals

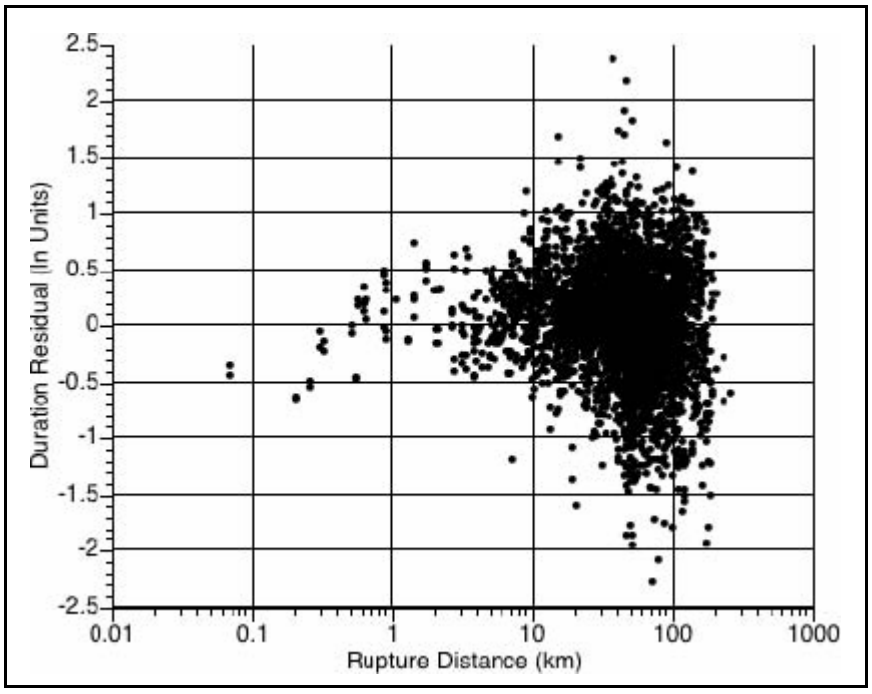

Figure 2-15
Distance Dependence of the Uniform Duration Residuals

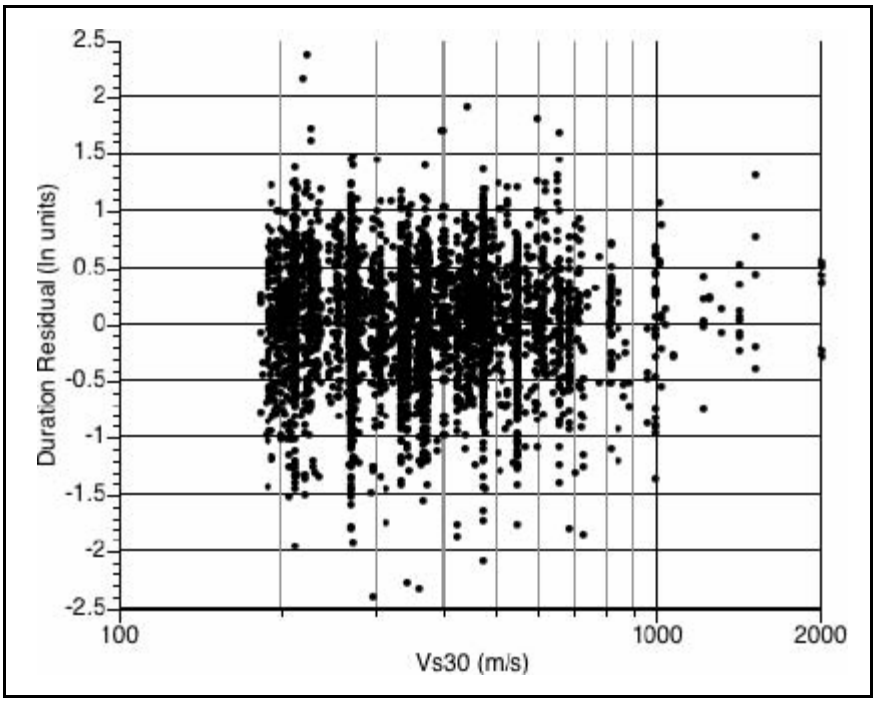

Figure 2-16
Shear-Wave Velocity Dependence of the Uniform Duration Residuals

Using the WUS based duration model, we then computed the duration residuals for CEUS/Canadian ground motions with PGA values greater than 0.05g. The duration residuals, shown in Figures 2-17, 2-18, and 2-19 as functions of the PGA, M, and Vs30 indicate that there is a bias toward negative residuals for earthquakes with moment magnitudes less than 5.0, and for PGA values less than 0.2g. The mean residual is –0.09 ± 0.10 which is not significantly different from zero. Therefore, based on the available CEUS data set, the WUS duration model is considered to be applicable to the CEUS. Since this conclusion is based on a small number of CEUS recordings, it should be confirmed if there is a significant increase in the number of available CEUS strong ground motion data in the future.

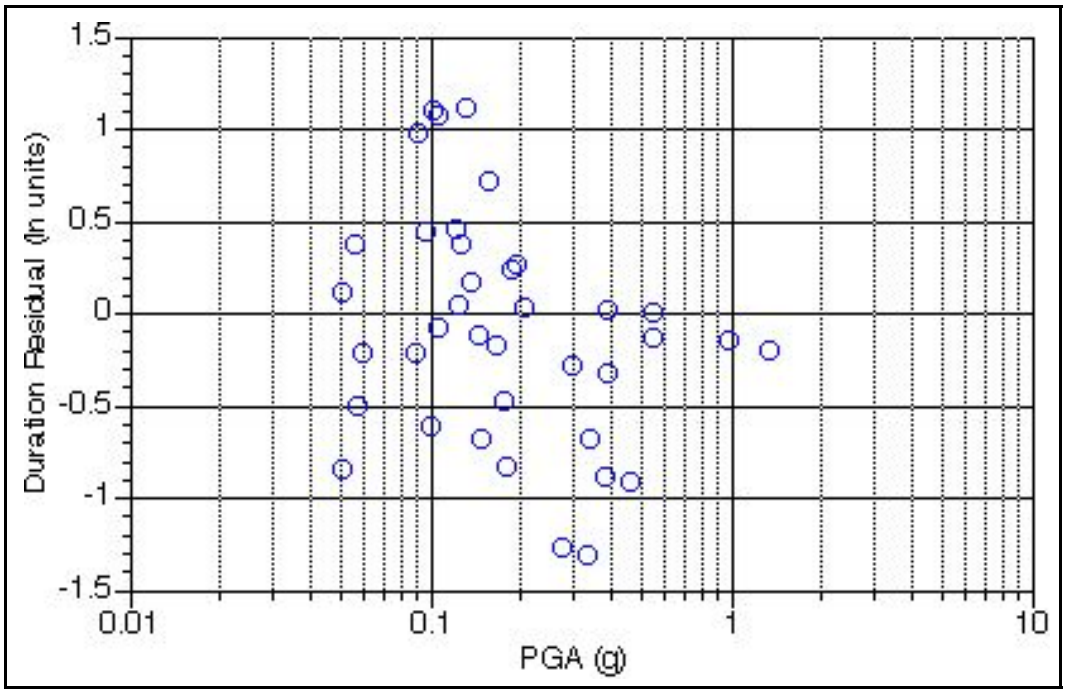

Figure 2-17
PGA Dependence of the Uniform Duration Residuals from the CEUS Ground Motions Listed in Table 2-2

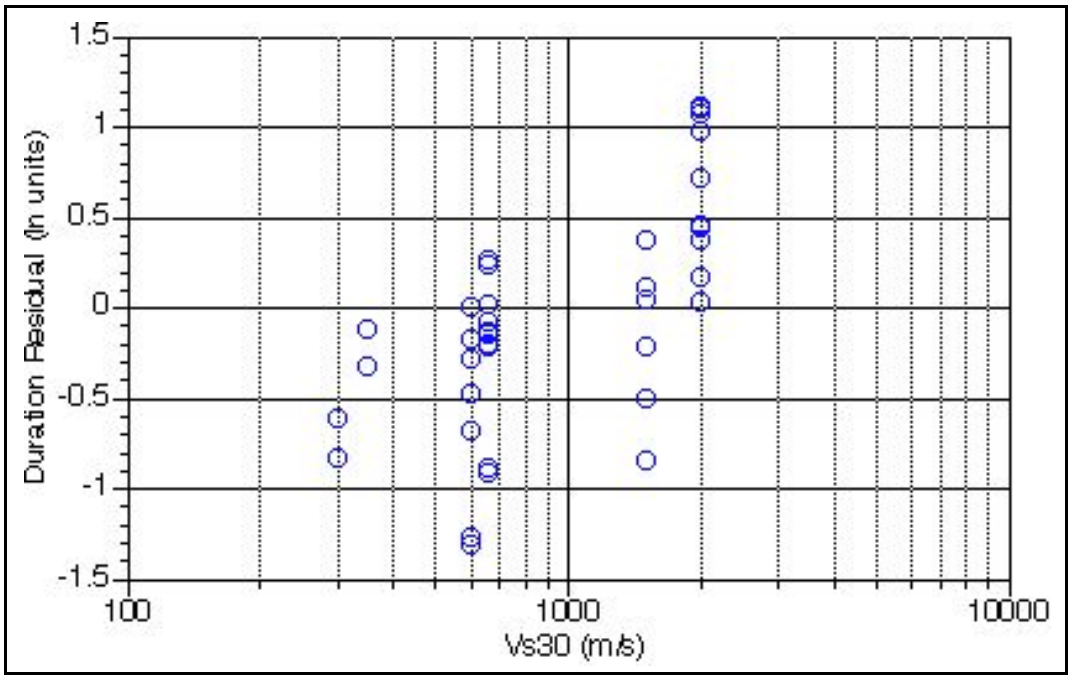

Figure 2-18
Magnitude Dependence of the Uniform Duration Residuals from the CEUS Ground Motions Listed in Table 2-2

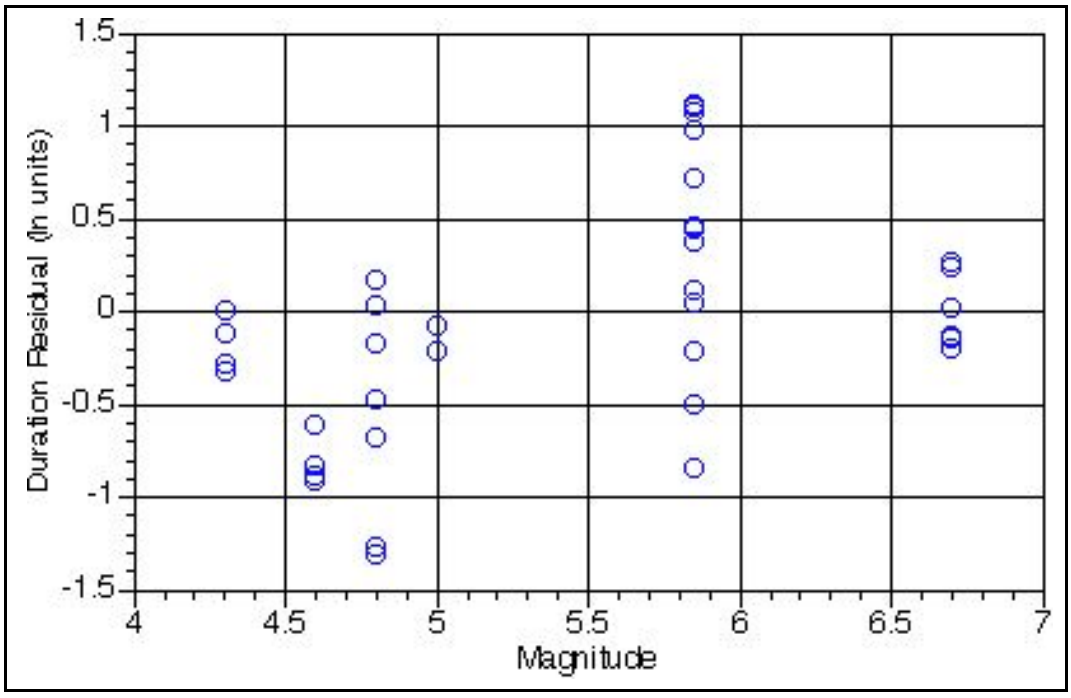

Figure 2-19
Vs30 Dependence of the Uniform Duration Residuals from the CEUS Ground Motions Listed in Table 2-2

Model for CAV

To apply the CAV model, the median from the duration model is used in eq. 2-1 and 2-2 rather than the duration of the recorded ground motions. If the duration is estimated using eq. 2-2 or 2-3, then the total standard deviation of the ln(CAV) model (given the PGA. M, and V_{s30}) is given by

$$\sigma_{\ln CAV} = \sqrt{\left(c_8 + 2c_9 \ln(D\hat{u}r_{uni})\right)^2 \sigma^2_{\ln dur} + \sigma^2_{\ln CAV_1}} \qquad \textbf{(Equation 2-3)}$$

where $\sigma_{\ln CAV_1}$ is the standard deviation of the ln(CAV) model from eq. 1-1 (e.g., based on the observed durations). The total standard deviation is shown in Figure 2-20 as a function of the median duration.

The residuals of EUS CAV computed using the median durations are shown in Figure 2-21. The mean residual is 0.06 ± 0.09. There is a trend that the model over predicts the CAV values for PGA values greater than 0.2g.

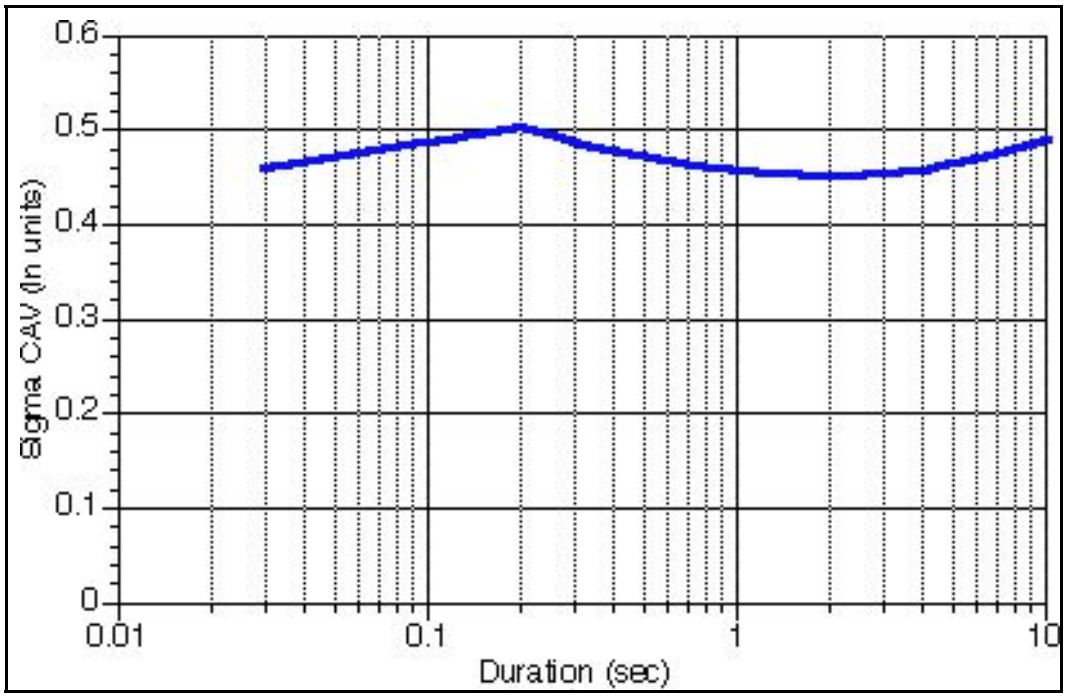

Figure 2-20
Standard Deviation of the ln(CAV) if the Median Duration Model is Used

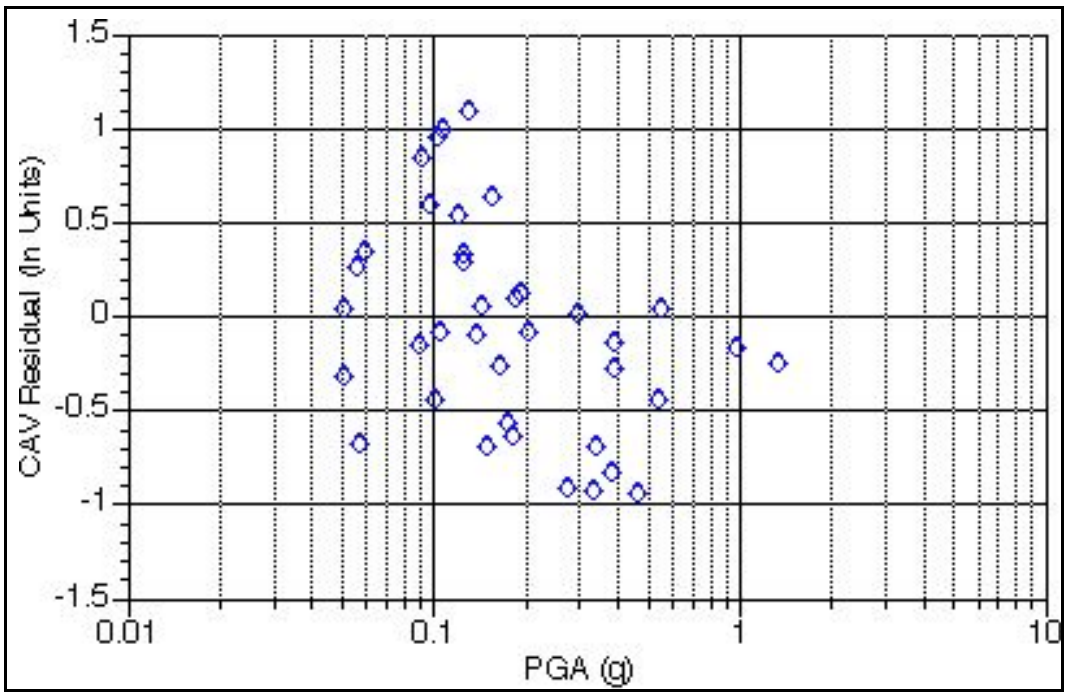

Figure 2-21
EUS CAV Residuals Using the EUS Duration Model

Probability of Exceeding Specified CAV Value

The probability of exceeding a CAV value of 0.16g-sec is given by

$$P(CAV > 0.16g - s \mid PGA, M, V_{s30}) = \begin{cases} 1 - \Phi(\varepsilon^*_{CAV}) & for PGA \geq 0.025g \\ 0 & for PGA < 0.025g \end{cases} \quad \textbf{(Equation 2-4)}$$

where Φ is the cumulative normal distribution and ε^*_{CAV} is the number of standard deviations in the CAV model that will yield 0.16g-sec. That is,

$$\varepsilon^*_{CAV} = \frac{\ln(0.16) - \ln CAV(PGA, M, V_{s30}, D\hat{u}r(PGA, M, V_{S30}))}{\sigma_{\ln CAV}} \quad \textbf{(Equation 2-5)}$$

where the CAV is given by eq. 2-1 and $\sigma_{\ln CAV}$ is given by eq. 2-3. The probability of exceeding a CAV value of 0.16 g-s is shown in Figure 2-22.

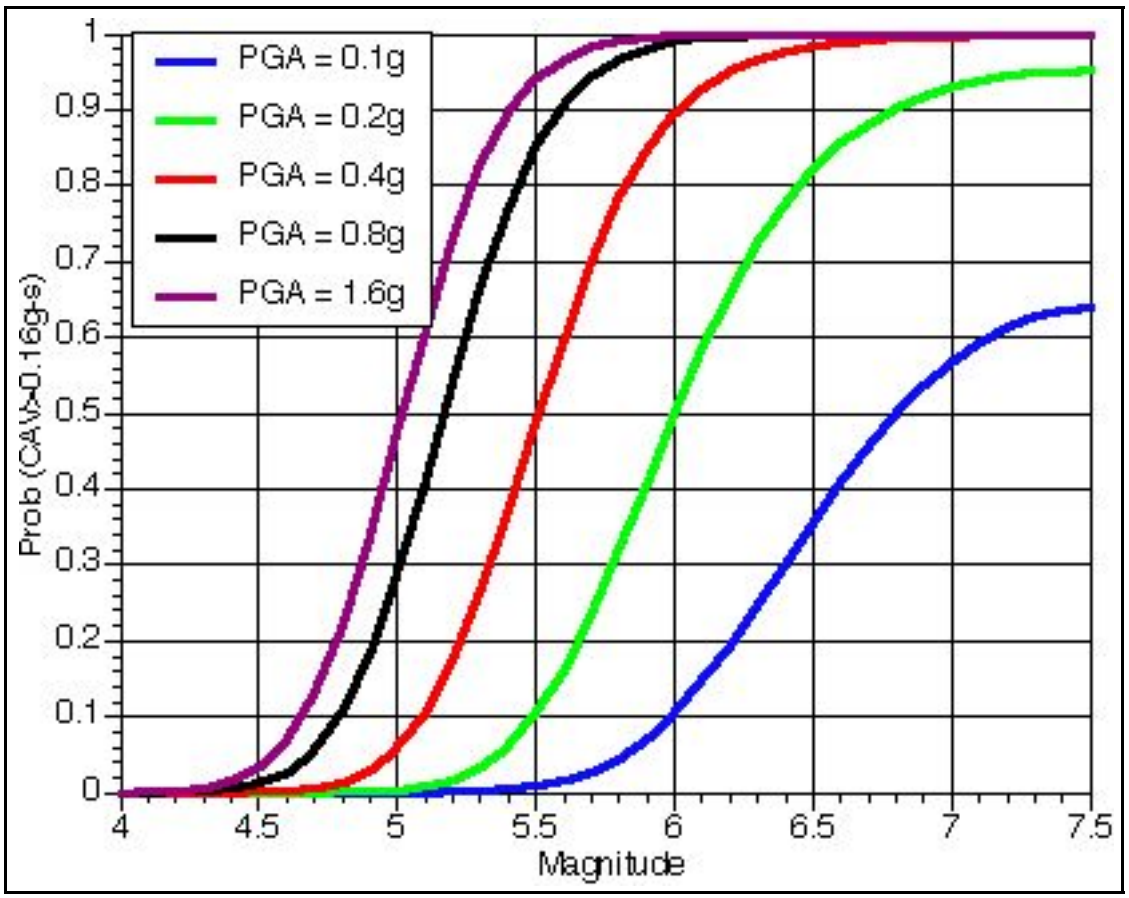

Figure 2-22
Probability of CAV>0.16g-sec

3
APPLICATION OF THE CAV MODEL FOR RESPONSE SPECTRAL VALUES

The CAV model described above is based on the PGA. To estimate the effect of CAV on the response spectral values at periods other than 0 (e.g., other than PGA) requires a model of the relation between the PGA and the spectral acceleration. The spectral shape from the attenuation relation can be used to estimate the median PGA given the median spectral acceleration. In addition to the median spectral shape, we need to account for the aleatory variability of the spectral shape. Models for the correlations of the normalized residuals (epsilon values) of PGA and spectral acceleration from attenuation relations are developed.

Assuming a linear correlation, the relation between the residuals is given by:

$$\varepsilon_{SA}(f) = b_1 \varepsilon_{PGA} \qquad \textbf{(Equation 3-1)}$$

where ε_{PGA} is the epsilon value of PGA for the time series and $\varepsilon_{SA}(f)$ is the epsilon value of spectral acceleration at frequency *f*. The dataset used to develop the correlation model is the PEER NGA data set, with residuals calculated using a preliminary version of the Abrahamson and Silva (2005) model. The model coefficients were estimated using ordinary least-squares. The resulting coefficients can be found in Table 3-1. At high frequencies, the WUS b_1 values are close to unity because the WUS data does not have much high frequency content. For the EUS data with greater high frequency content, the correlation was estimated using the variability of the spectral shapes from the Saguenay earthquake data (Table 3-1).

Table 3-1
Coefficients for the Correlation of ln(PGA) and ln(Sa)

	WUS	EUS
Freq (Hz)	b_1	b_1
0.5	0.590	0.50
1	0.590	0.55
2.5	0.600	0.60
5	0.633	0.75
10	0.787	0.88
20	0.931	0.90
25	0.956	0.91
35	0.976	0.93

The median Sa for a given PGA value is given by:

$$\ln\left(Sa(f) \mid PGA, M, R, V_{S30}\right) = \ln\left(Sa_{med}(M, R, V_{s30}, f)\right) + b_1(f)\varepsilon_{PGA}\sigma_{\ln SA} \quad \textbf{(Equation 3-2)}$$

The standard deviation of ln(Sa(f)|PGA) is given by:

$$\sigma_{\ln Sa|PGA} = \sqrt{1 - b_1^2}\,\sigma_{\ln Sa} \quad \textbf{(Equation 3-3)}$$

4

METHODOLOGY FOR APPLICATION OF MINIMUM CAV IN SEISMIC HAZARD ANALYSES

The CAV models given above can be easily used to modify the results from a standard hazard analysis to remove the earthquakes that have no damage potential. The CAV filtering can be applied as part of the hazard analysis (e.g., inside the hazard integral) or it can be applied as a post process. These two approaches are discussed below.

Application of CAV Filtering During the Hazard Calculation

The most direct method for applying the minimum CAV model described above as part of the hazard calculation is to add an integral over the PGA aleatory variability. This becomes

$$\nu(Sa>z)=\sum_{i=1}^{N_{source}} N_i(M>M_{\min}) \int_{M=M_{\min}}^{M_{\max i}} \int_{R=0}^{\infty} \int_{\varepsilon_{PGA}=-5}^{5} \begin{matrix} f_{mi}(M)\, f_{ri}(r,M)\, f_{\varepsilon}(\varepsilon_{PGA}) \\ P\left(CAV>0.16 \mid M,PGA(M,R,\varepsilon_{PGA})\right) \\ P(Sa>z \mid M,R,PGA)\, d\varepsilon_{PGA}\, dr\, dM \end{matrix} \quad \textbf{(Equation 4-1)}$$

where P(CAV>0.16|M,PGA) is given by eq. 2-4,

$$P(Sa>z \mid M,R,PGA)=1-\Phi(\varepsilon_{SA}^{'}) \quad \textbf{(Equation 4-2)}$$

and

$$\varepsilon_{Sa}^{'}=\frac{\ln(z)-\left(\ln Sa_{med}(M,R)+b_1\varepsilon_{PGA}\sigma_{SA}\right)}{\sqrt{1-b_1^2}\,\sigma_{SA}} \quad \textbf{(Equation 4-3)}$$

For large hazard calculations, this additional integral may add significantly to the computation time. A more computationally efficient method for applying the minimum CAV in a PSHA could be developed that avoids the need for the additional integral in the hazard if deemed necessary to minimize computer run time.

Application of CAV Filtering in the Post Processing of the Hazard Calculation

A standard hazard analysis will yield a hazard curve, $\nu(Sa_{Rock}(f)>z_k)$, and the deaggregation, $Deagg(M_i<M<M_{i+1},\ R_j<R<R_{j+1} Sa(f)>z_k)$. Using these two pieces of information, we can compute the rate of occurrence of spectral acceleration over a small acceleration range from a specified magnitude and distance range:

$$\nu(z_k < Sa_{Rock}(f) < z_{k+1}, M_i < M < M_{i+1}, R_j < R < R_{j+1}) =$$
$$\nu(Sa_{Rock}(f) > z_k) Deagg\left(M_i < M < M_{i+1}, R_j < R < R_{j+1}, z_k\right)$$
$$-\nu(Sa_{Rock}(f) > z_{k+1}) Deagg\left(M_i < M < M_{i+1}, R_j < R < R_{j+1}, z_{k+1}\right) \quad \textbf{(Equation 4-4)}$$

For more compact notation, this rate of occurrence is denoted as $\nu_{occur}(z_k,M_i,R_j)$.

Let ν' be the hazard curve for potentially damaging ground motions (CAV>0.16g-sec), then

$$\nu'(Sa_{Rock}(f) > z_n) = \sum_{i=1}^{N_m} \sum_{j=1}^{N_r} \sum_{k=n}^{N_a} \nu_{occur}(z_k, M_i, R_j) P(CAV > 0.16g - s \mid z_k, M_i, R_j) \quad \textbf{(Equation 4-5)}$$

In words, the CAV filtering of the hazard is implemented by first breaking the hazard curve back down into rates of occurrence of scenario earthquakes (M,R,Sa). From this scenario earthquake, we can compute the epsilon for the given Sa. From this information, we can then compute the probability that this scenario will lead to a CAV value greater than 0.16g-sec. This probability is then multiplied by the rate of the scenario. We then sum up the rates of all the scenarios with spectral accelerations greater than our test value, resulting in the CAV filtered hazard.

The hazard curves described above are for “outcropping rock”. However, the CAV model was developed using surface ("soil" or "rock") values of spectral acceleration. When calculating the probability of CAV>0.16g-sec it is necessary to amplify the $Sa_{Rock,k}$ to $Sa_{Soil,k}$ for the site, and use the $Sa_{Soil,k}$ values as input to the CAV model since the CAV model was developed for surface ground motions.

5
EXAMPLE APPLICATION

As an example, the CAV filtered hazard is computed for a CEUS rock site using the USGS (Frankel et al. 2002) smoothed seismicity and the Toro et al (1997) attenuation relation. No fault sources were included. In this example, the CAV filtering is applied inside the hazard integral using equations 4-1, 4-2, and 4-3.

The hazard curves for 20 Hz spectral acceleration are shown in Figure 5-1 with and without the CAV filtering. The effect of removing the events with CAV less than 0.16g-sec is to flatten the hazard curve at small ground motion levels. There is little effect on the hazard curve for high ground motion levels since these levels will be associated with CAV values greater than 0.16g-sec. The uniform hazard spectrum for a probability level of 1E-4 is shown in Figure 5-2 with and without the CAV filtering. At a hazard level of 1E-4, the UHS is reduced by about 10-25% due to CAV filtering. This example is for a site that is not close the either the Charleston or New Madrid sources. For sites close to these sources, the effect of the CAV filtering on the low frequency part of the Uniform Hazard Spectrum (UHS) will be smaller since the ground motions form these larger magnitude earthquakes will have large CAV values.

The deaggregation for 20 Hz spectral acceleration for a hazard level of 1E-4 is shown in Figure 5-3 with and without the CAV filtering. The effect of the CAV filtering is to remove the contribution from smaller magnitudes, shifting the peak in the deaggregation to larger magnitudes and larger distances. For the PSHA using a fixed lower bound moment magnitude of 4.6, there is a significant contribution from **M**4.6-5.0, but these are removed in the CAV filtered hazard.

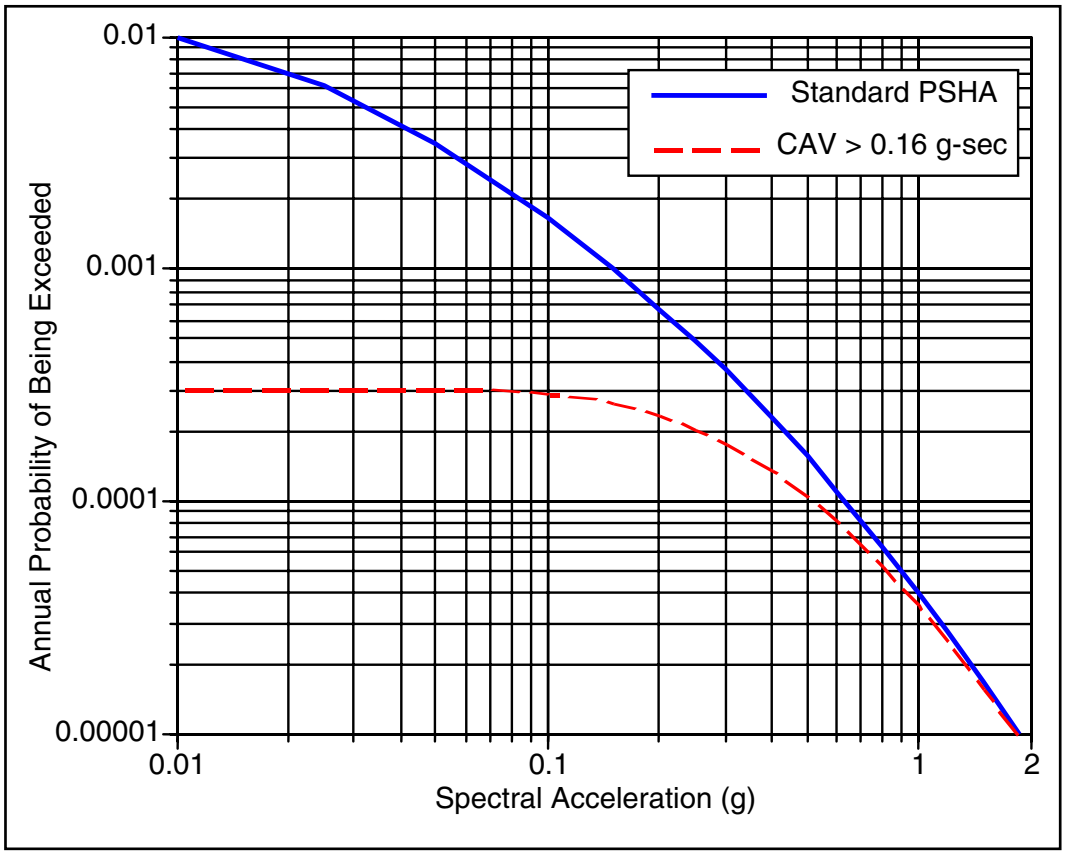

Figure 5-1
20 Hz Hazard Computed With and Without CAV Filtering

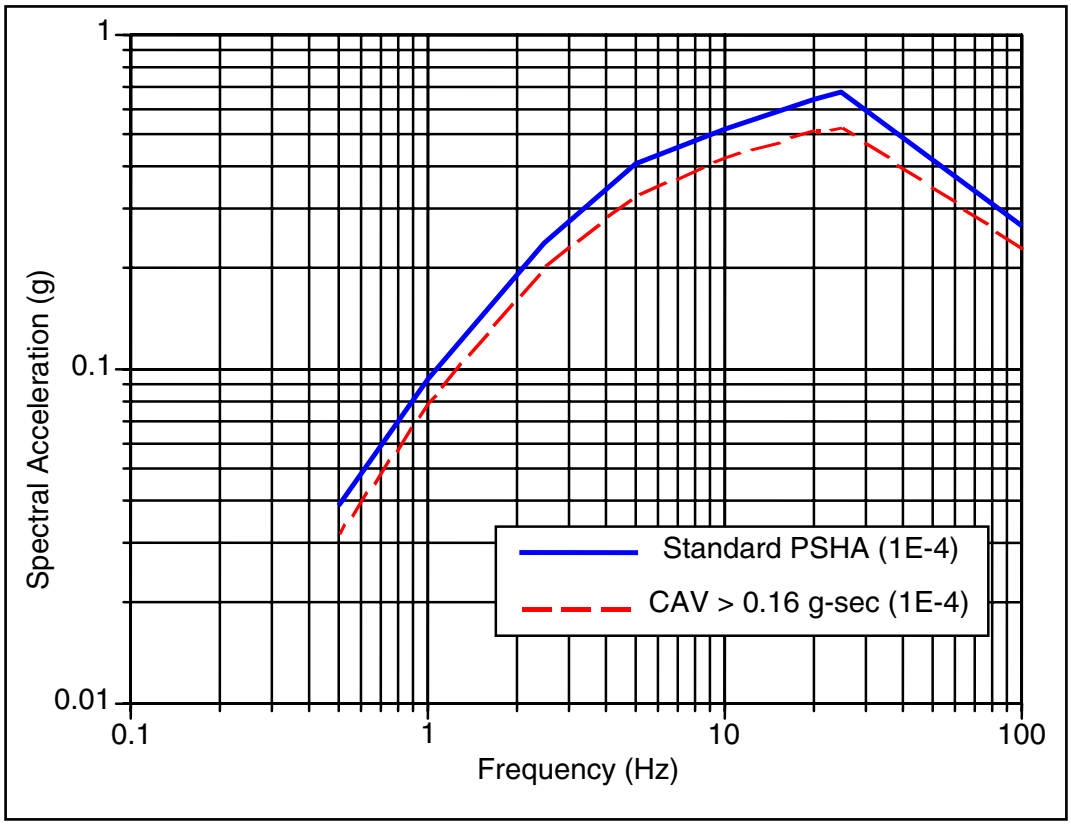

Figure 5-2
UHS for 1E-4 With and Without CAV Filtering

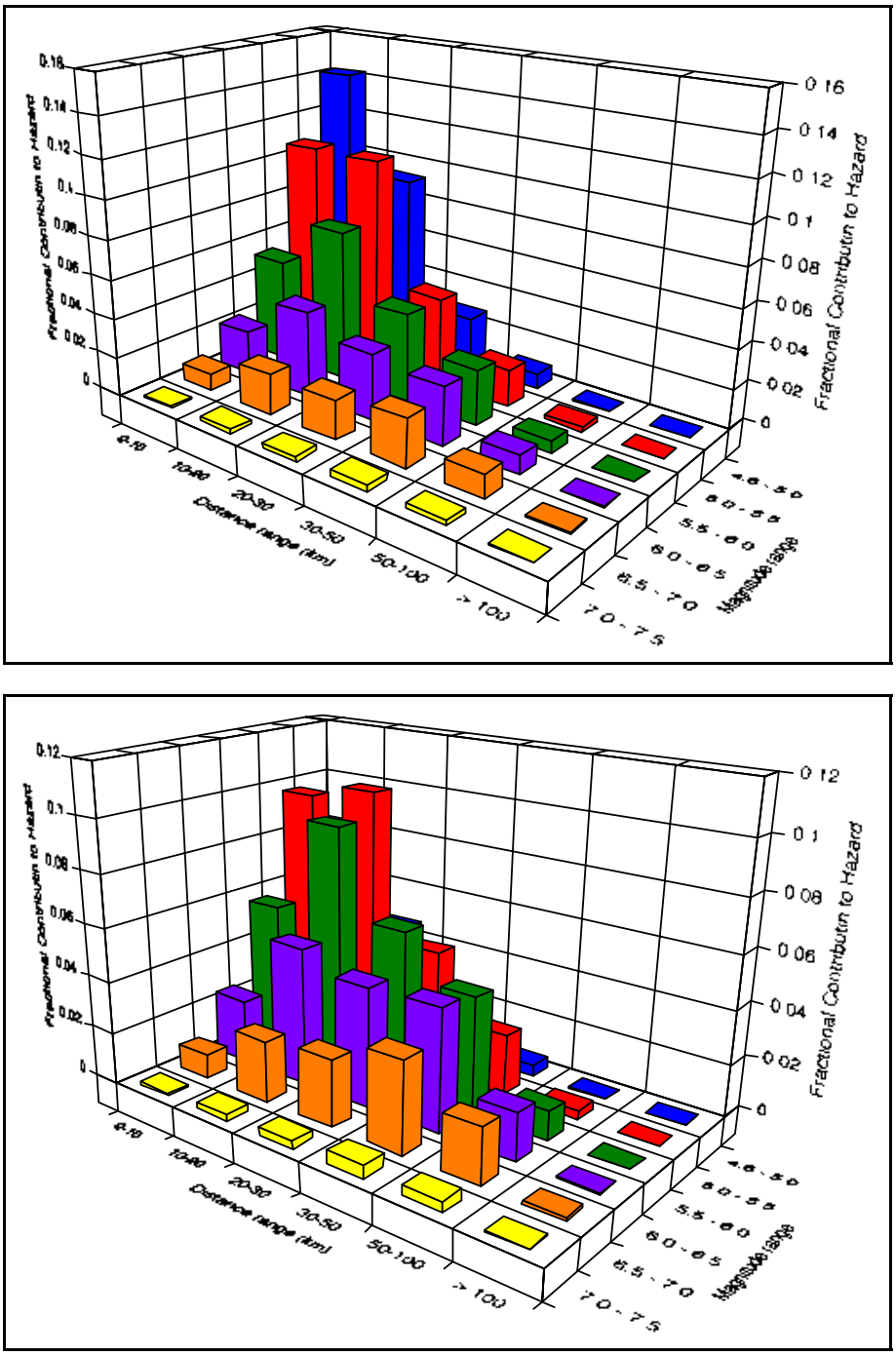

Figure 5-3
Deaggregation of 20 Hz Spectral Acceleration Hazard for 1E-4
The upper plot is the standard PHSA. The lower plot is the CAV filtered deaggregation.

6
CONCLUSIONS

This study provides the technical basis for establishing the appropriate distribution of low magnitude earthquakes for use in probabilistic seismic hazard computations for nuclear power plant applications. Current seismic hazard methods generally utilize a lower bound body wave magnitude cut-off value of 5.0 (approximate moment magnitude of 4.6) to integrate the probabilistic seismic hazard. This lower bound magnitude cut-off level was a conservatively defined value based on several past research studies whose objective was to estimate the damage potential of small earthquakes. A much more complete and technically defendable characterization of the damage potential for small earthquakes was determined to be the cumulative absolute velocity (CAV). A CAV value of 0.16 g-sec was defined in past studies to characterize a conservative estimate of the threshold between damaging earthquake motions and non-damaging earthquake motions for buildings of good design and construction as defined by the Modified Mercalli Scale. Based on the review of available CEUS and WUS data, CAV is modeled as a function of the uniform duration, magnitude, peak ground acceleration, and site shear wave velocity. The application of a minimum CAV value significantly reduces the contribution of small magnitude earthquakes to the total hazard leads to a controlling earthquake that more correctly represents the contributions of potentially damaging earthquakes to the hazard at a site. At high frequencies, the magnitude of the controlling earthquake increases from near magnitude 5.25 for the fixed lower bound moment magnitude 4.6 to magnitude 5.8 by applying the CAV model.

7
REFERENCES

Abrahamson, N. A. and W. J. Silva (2005). Preliminary results of the A&S 2005 attenuation relation, presented at the USGS workshop on Attenuation Relations to be used in the USGS National Seismic Hazard Maps, Menlo Park, CA, October 24, 2005,

Bolt, B.A. (1973). *Duration of Strong Ground Motion,* Proc. Fifth World Conf. Earth. Eng., Rome, 1304-1307.

EPRI (1993). Guidelines for Determining Design Basis Ground Motions, EPRI Report TR-102293, November 1993.

Frankel, A.D., Petersen, M.D., Muller, C.S., Haller, K.M., Wheeler, R.L., Leyendecker, E.V., Wesson, R.L., Harmsen, S.C., Cramer, C.H., Perkins, D.M., and Rukstales, K.S., (2002), Documentation for the 2002 Update of the National Seismic Hazard Maps: U.S. Geological Survey, Open-File Report 02-420.

McCann, M.W. and J.W. Reed (1989). *Proceedings: Engineering Characterization of Small-Magnitude Earthquakes*, EPRI Report NP-6389, June 1989.

National Earthquake Information Center (2005). http://neic.usgs.gov, 2005.

O'Hara, T.F. and J.P. Jacobson (1991). Standardization of the Cumulative Absolute Velocity, EPRI Report TR-100082, Tier 2, December 1991.

PEER (2005) NGA Strong Motion Database. http://peer.Berkeley.edu/NGA, 2005.

Reed, J.W. and R.P. Kennedy (1988). *A Criterion for Determining Exceedance of the Operating Basis Earthquake*, EPRI Report NP-5939, July 1988.

Toro, G.R., N.A. Abrahamson, and J.F. Schneider (1997). *Model of Strong Ground Motions from Earthquakes in Central and Eastern North America: Best Estimates and Uncertainties*, Seism. Res. Let., 68, 58-73.

Export Control Restrictions

Access to and use of EPRI Intellectual Property is granted with the specific understanding and requirement that responsibility for ensuring full compliance with all applicable U.S. and foreign export laws and regulations is being undertaken by you and your company. This includes an obligation to ensure that any individual receiving access hereunder who is not a U.S. citizen or permanent U.S. resident is permitted access under applicable U.S. and foreign export laws and regulations. In the event you are uncertain whether you or your company may lawfully obtain access to this EPRI Intellectual Property, you acknowledge that it is your obligation to consult with your company's legal counsel to determine whether this access is lawful. Although EPRI may make available on a case-by-case basis an informal assessment of the applicable U.S. export classification for specific EPRI Intellectual Property, you and your company acknowledge that this assessment is solely for informational purposes and not for reliance purposes. You and your company acknowledge that it is still the obligation of you and your company to make your own assessment of the applicable U.S. export classification and ensure compliance accordingly. You and your company understand and acknowledge your obligations to make a prompt report to EPRI and the appropriate authorities regarding any access to or use of EPRI Intellectual Property hereunder that may be in violation of applicable U.S. or foreign export laws or regulations.

The Electric Power Research Institute (EPRI)

The Electric Power Research Institute (EPRI), with major locations in Palo Alto, California, and Charlotte, North Carolina, was established in 1973 as an independent, nonprofit center for public interest energy and environmental research. EPRI brings together members, participants, the Institute's scientists and engineers, and other leading experts to work collaboratively on solutions to the challenges of electric power. These solutions span nearly every area of electricity generation, delivery, and use, including health, safety, and environment. EPRI's members represent over 90% of the electricity generated in the United States. International participation represents nearly 15% of EPRI's total research, development, and demonstration program.

Together…Shaping the Future of Electricity

Printed on recycled paper in the United States of America

1012965

ELECTRIC POWER RESEARCH INSTITUTE

3420 Hillview Avenue, Palo Alto, California 94304-1395 • PO Box 10412, Palo Alto, California 94303-0813 • USA
800.313.3774 • 650.855.2121 • askepri@epri.com • www.epri.com